Addressing the problem of uniform converging spherical shock wave in water

M. Nitishinskiy, S. Efimov, D. Yanuka, V. Tz. Gurovich, and Ya. E. Krasik

Physics Department, Technion, Haifa 32000, Israel

Time-resolved parameters of plasma compressed by a shock wave generated by the underwater electrical explosion of a spherical wire array are presented. The plasma was preliminarily formed inside a capillary placed at the equatorial plane along the axis of the array. Temporal evolution analysis of H_α and C II spectral lines showed that the plasma density increases from its initial value of $\sim 3 \times 10^{17}\,cm^{-3}$ up to $\sim 5.5 \times 10^{17}\,cm^{-3}$ within 300 ± 25 ns. These results were found to be in agreement with those of the model that considers the adiabatic compression of the plasma by the converging capillary walls caused by interaction with the incident shock wave with a pressure of $\sim 3 \times 10^9\,Pa$ at a radius of 1.5 mm. The latter results coincide well with those of the 1D hydrodynamic modeling, which assumes uniformity of the converging shock wave. *Published by AIP Publishing.*
[http://dx.doi.org/10.1063/1.4964286]

I. INTRODUCTION

Converging shock waves can be used efficiently for the research of extreme state of matter and various applications.[1–5] Recent experimental and numerical research of strong shock wave (SSW) generation and convergence using underwater electrical explosion of a spherical wire array showed that it is possible to form an extreme state of water in the vicinity of the SSW implosion using rather moderate pulse power current generators.[4] However, the uniformity of the SSW convergence, which determines the maximal achievable pressure behind the SSW front, remains questionable. The common approach for obtaining the parameters of the water behind the SSW front is to use the measured SSW velocity[5] coupled with the equation of state (EOS) and Rankine–Hugoniot relations, which allows one to calculate pressure, density, and temperature at that location. However, in the case of a converging spherical shock wave, images of the SSW front captured at different times of the wave implosion cannot be registered, and thus, other diagnostic methods have to be sought.

In earlier studies,[6,7] the results of studies of the parameters of the plasma formed in the capillary placed along the axis of the equatorial plane of the spherical wire array were used to reconstruct the parameters of the incident SSW. A copper capillary preliminarily filled with air[6] or a quartz capillary filled with C_3H_8 gas[7] were used in these experiments. In the latter case, the plasma was formed in the capillary by the gas discharge prior to the SSW interaction with the capillary. It was shown that when the SSW propagating in water and interacting with the capillary reaches its inner wall, intense partial evaporation and ionization of wall material occur (spectral lines of Cu I and Si II were obtained). The plasma electron density was determined by analyzing the Stark broadening of the spectral lines, and the plasma electron temperature was calculated from the ratio of the spectral lines' intensities.[7] It was found that the preliminarily formed plasma is characterized by density and temperature of $\sim 2 \times 10^{17}\,cm^{-3}$ and ~ 3.8 eV,

respectively. Further, because of the compression of the plasma by imploding capillary, plasma density and temperature reach $\sim 5 \times 10^{17}\,cm^{-3}$ and ~ 4.2 eV, respectively. These data were used to estimate the incident SSW pressure at the water–capillary boundary. However, in these experiments, the plasma parameters were obtained almost without time resolution (averaged along ~ 500 ns).

In the present study, we overcame this disadvantage, and the parameters of the plasma compressed in the capillary were determined with a time resolution of 2 ns. This allowed us to determine the evolution of the plasma implosion in the capillary and to derive the velocity of implosion at the inner capillary wall ($R = 1$ mm). Using the value of this velocity, the SSW pressure at the outer wall of the capillary was determined. The latter was found to be in good agreement with the results of one-dimension hydrodynamic calculations coupled with the EOS of water, which consider uniform convergence of the SSW.

II. EXPERIMENTAL SETUP AND DIAGNOSTICS

A detailed description of the experimental setup was presented in Ref. 7. The setup consists of a high-current generator (3.6 kJ of stored energy), an experimental chamber filled with de-ionized water, a 30 mm diameter spherical wire array, and diagnostics. The wire array, consisting of 40 Cu wires each 100 μm in diameter, was placed inside the experimental chamber between high-voltage and grounded electrodes. Plasma in the vicinity of the sphere origin was generated by the electrical discharge in C_3H_8 gas (pressure of ~ 40 Pa) between two electrodes (gap of ~ 2 mm) placed inside a quartz capillary, the outer and inner diameters of which were 3 mm and 2 mm, respectively. The capillary was installed in the equatorial plane along the sphere's axis and preliminarily evacuated to a pressure of ~ 0.2 Pa. The location of the capillary at that position does not influence significantly the convergence of the SSW. Indeed, in our earlier research[4] the damages of the capillary were obtained exactly
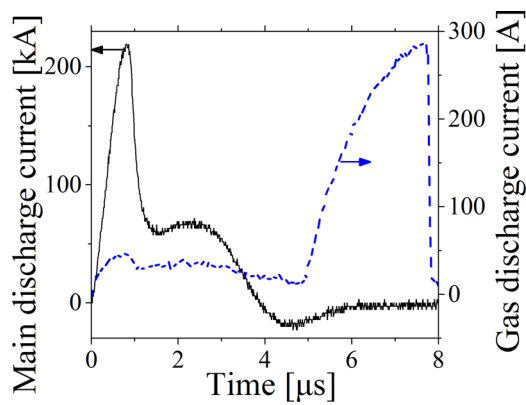
FIG. 1. Typical waveforms of the main discharge current (solid line) and the current between the two electrodes placed inside the capillary (dashed line).

in the vicinity of the implosion origin, as well as the time-of-flight data of the SSW with and without the capillary was almost the same, i.e., within the error bar related mainly to the time jitter in the explosion of the wire array.

To generate the plasma between the electrodes, a voltage pulse with an amplitude up to 13 kV was applied. Typical waveforms of the main discharge current applied to explode the wire array and the current pulse used to generate plasma inside the capillary are shown in Fig. 1.

The application of the main discharge current causes the electrical explosion of the wires and the generation of single shock waves, which overlap and form a converging SSW. The interaction of this SSW with the capillary, where the preliminary plasma was formed by an additional discharge, results in fast changes in the plasma parameters, which were studied using time-resolved optical emission spectroscopy (OES). The visible light emission from this plasma was transferred to the optical diagnostic scheme using optical fiber installed inside one of the electrodes at a distance of ~1.5 mm from the sphere origin. This fiber collected the light emission from the volume with a diameter which roughly coincided with the inner diameter of the capillary (see Fig. 2). The light collected from the fiber's output was focused by a system of lenses, beam-splitters, and mirrors to the inputs of two spectrometers and to a single photomultiplier tube (PMT). A Chromex-500 spectrometer (0.5 m focal length, 300–1800 grooves/mm) with a cylindrical lens and linear fiber bundle array coupled with a 9-channel PMT array at its output was used to study the temporal evolution
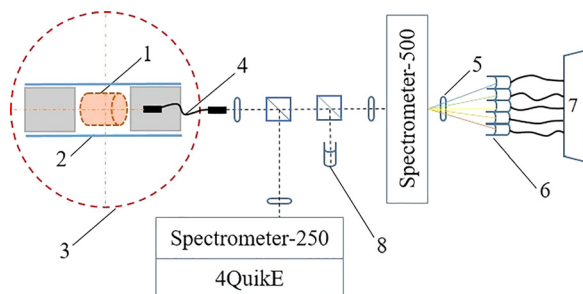

FIG. 2. Optical diagnostic scheme. 1—plasma; 2—capillary; 3—spherical wire array; 4—optical fiber; 5—cylindrical lens; 6—fiber bundle array; 7–9—channel PMT array; and 8—single PMT.

of the spectral lines' intensity. The fiber bundle array consisted of 9 bundles with 91 fibers in each. The light from each bundle carrying a certain spectral interval was coupled with a Hamamatsu H10721-01 PMT. Signals from these 9 PMTs were recorded by Tektronix TDS 784A oscilloscopes (1 GHz, 4 GS/s), allowing us to record spectral lines with nanosecond time scale resolution. The spectral resolution of the optical setup was varied by changing the grating of the spectrometer and the positions of the cylindrical lens and fiber array, and measured using Oriel spectral calibration lamps. The total spectral range obtained by the PMT array was either 21 Å for the observation of the C II (4267 Å) and C III lines (4647 Å), resulting in a spectral resolution of 2.6 Å/PMT, or 56 Å in the case of the H_α (6563 Å) spectral line observation, corresponding to a 7 Å/PMT spectral resolution.

A Chromex-250 spectrometer (0.25 m focal length, 1800 grooves/mm) with a 4QuikE camera (frame duration of 500 ns) was used for monitoring the time-integrated intensity of the same spectral line. The single PMT (Hamamatsu R7400U-04) was used to study the temporal evolution of the plasma light emission intensity. In these experiments, the shapes and intensities of the spectral lines emitted by the capillary plasma were studied without the wire array explosion (that is, with only the capillary plasma discharge) and with the explosion of wires accompanied by converging SSW generation.

III. EXPERIMENTAL RESULTS

The H_α, C II, and C III spectra of line profiles obtained prior to and during the SSW interaction with the capillary were fitted using a Voigt function. Here, the Stark effect was considered to be responsible for the Lorentzian component of the broadening (the Doppler broadening of the spectral lines was neglected at this spectral resolution).

The plasma electron density was determined from the H_α spectral line broadening using tabulated data[8] for plasma electron temperature $T_e \cong 3$ eV.[7] The evolution of the plasma electron density also was studied using the data[9] for C II spectral line broadening, but with less accuracy, because the broadening of the C II spectral lines was significantly less than that of the H_α spectral line. Here, let us note that in one generator shot, only one spectral line was obtained; therefore, at least four shots for each spectral line measurements were performed.

Typical time-dependent spectral line intensities of the excited hydrogen and C II and C III ions are shown in Fig. 3. Here, time $t = 0$ corresponds to the beginning of the discharge current, and the explosion of the wires (i.e., the time when the discharge current through the wires reaches its maximal amplitude, after which a fast current decay begins) occurs at 0.95 ± 0.1 μs. One can see that a gradual increase in both the intensity and full width at half maximum (FWHM) of these spectral lines begins at $t > 6.8$ μs. At $t > 7.2$ μs, this increase becomes significantly faster and at $t \approx 7.3$ μs one obtains maximal intensities (Figs. 3(a) and 3(b)). Later, the intensity of the spectral lines decreases together with significant increases in the intensity of the continuum spectrum (Fig. 3(b)). This
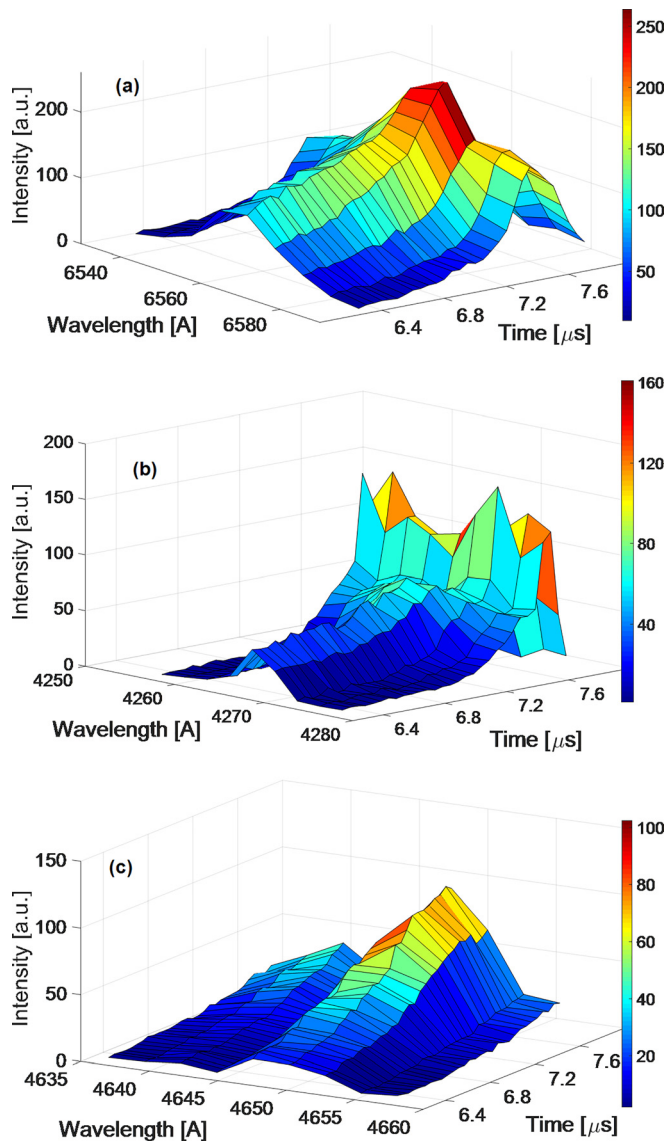
FIG. 3. Time evolution of H_α (a), C II (b), and C III (c) spectral lines.
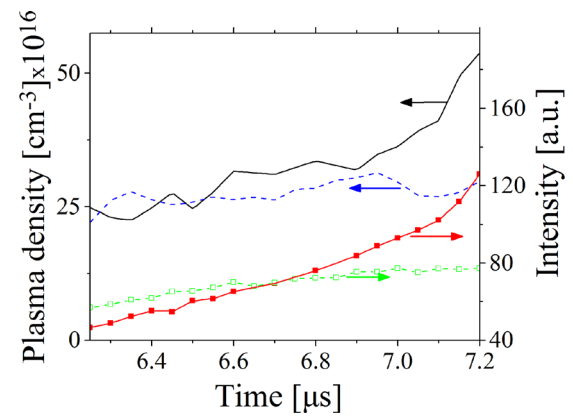

FIG. 4. Time-dependent evolution of the H_α spectral line intensity and plasma electron density without (dashed lines) and with wire array explosion (solid lines).

showed similar results. Namely, the density of the preliminarily formed plasma is $(3.8 \pm 1.0) \times 10^{17}\,\mathrm{cm}^{-3}$ at $t < 6.85\,\mu s$. Further, the plasma density increases up to $5.5 \times 10^{17}\,\mathrm{cm}^{-3}$ with the increase in the spectral line intensity by a factor of 1.5. Later, i.e., at $t > 7.3\,\mu s$, also this line shows a decrease in intensity (see Fig. 3(b)) and the determination of its FWHM becomes questionable. One can see that the plasma density evolutions obtained by the analysis of H_α and C II spectral lines Stark broadening reasonably agree with each other. Continuum radiation was observed in all the shots with the wire array explosion and its light emission intensity became

time evolution of the spectral line intensities can be explained by the increase in density and temperature of the plasma as a result of its interaction with the converging SW and capillary walls.

The time evolution of the plasma density obtained from the analysis of H_α spectral line Stark broadening is shown in Fig. 4 together with the temporal evolution of this spectral line intensity. One can see that the intensities of the H_α spectral line and the plasma density without and with wire array explosion are almost the same at $t \leq 6.9\,\mu s$ and that the plasma can be characterized by the density $(2.8 \pm 0.5) \times 10^{17}\,\mathrm{cm}^{-3}$. Further, within 300 ns, the intensity of the spectral line increases 1.5 times and plasma density increases to above $5 \times 10^{17}\,\mathrm{cm}^{-3}$. However, later, i.e., at $t > 7.2\,\mu s$, the determination of the FWHM becomes problematic because of a fast increase in continuum radiation (see Fig. 3(a)).

The time-dependent evolution of the C II (4267 Å) spectral line intensity and plasma density together with the total intensity of the light emission obtained by the single PMT are shown in Fig. 5. Analysis of the Stark FWHM of this line
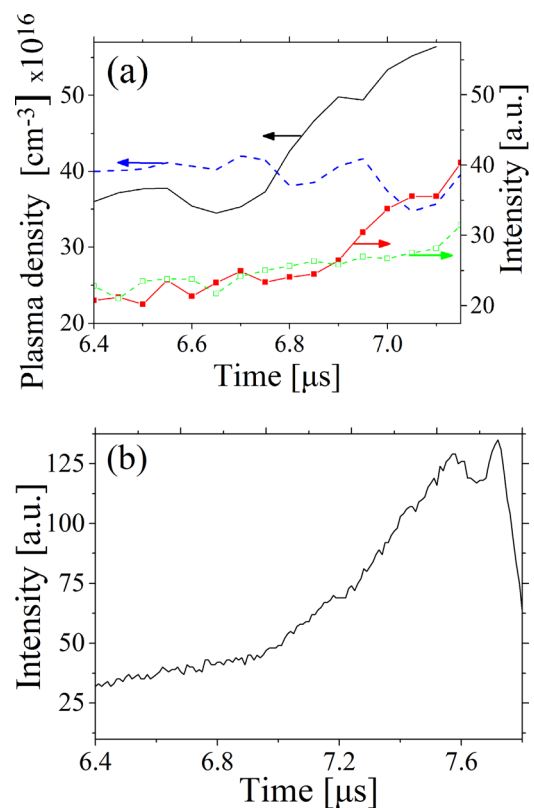

FIG. 5. Temporal evolution of (a) the C II (4267 Å) line intensity and plasma electron density without (dashed lines) and with wire array explosion (solid lines); (b) total light emission registered by a single PMT.

significant at $t = 7.2\,\mu s$ and reached its maximum intensity by $t_1 \sim 7.6 \pm 0.1\,\mu s$.

We observed also C III 4647 Å and 4651 Å spectral lines (see Fig. 3(c)), but these lines overlap with each other. Nevertheless, one can note (Fig. 6) that the time evolution of these lines' intensity follows that obtained for the H_α and C II spectral line intensity. In addition, one can see in Fig. 3(c) that at $t > 7.3\,\mu s$ the intensity of the C II 4639 Å spectral line becomes resolvable, indicating also an increase in the plasma density and temperature.

IV. DISCUSSION

The data obtained for the plasma parameters evolution can be used for estimating the pressure behind the front of the SSW interacting with the capillary. This value can be compared with the results of the 1D hydrodynamic modeling[10] coupled with EOS for water and considering uniform SW convergence.

Let us consider the following scenario of the SSW implosion. When the front of the converging SSW reaches the quartz capillary surface, a shock wave is generated in the capillary wall and propagates toward the axis. Behind the front of this shock wave, the capillary material also acquires a radial velocity toward the axis. Next, this shock wave reaches the inner capillary wall ($R_0 = 1\,mm$) at $t = t_0$. This leads to the formation of a reflecting wave in the quartz. The latter causes a partial evaporation of the capillary wall at that location and ionization of the evaporated atoms by the plasma electrons, leading to increase in the density of the preliminarily formed plasma. The wall's implosion with initial velocity U_0 results in an adiabatic compression of the plasma accompanied by an increase in its density and temperature. In addition, reflection of the shock wave from the inner surface of the wall is accompanied by the formation of a shock wave propagating in the preliminarily generated gas plasma. However, analysis[6] showed that this shock wave does not lead to significant compression and heating of the plasma and, therefore, its influence on the plasma parameters will be neglected. The experimental data presented in Sec. III can be used to determine the characteristic times of these processes and to estimate the value of U_0. The latter can be
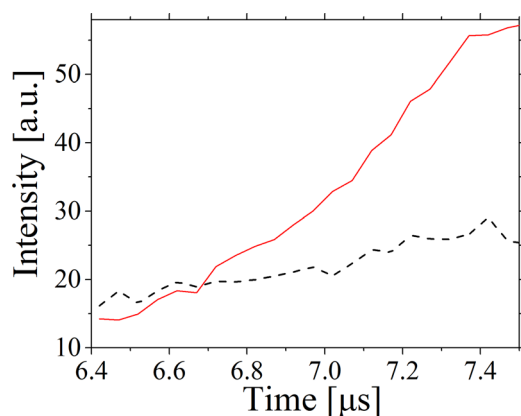

FIG. 6. C III spectral lines intensity temporal evolution without (dashed line) and with (solid line) wire array explosion.

compared with the results of the 1D hydrodynamic modeling, which assumes a uniform SSW convergence in water.

In experimental conditions, we were able to detect the time $t = t_0$ when the intensity of the plasma light emission becomes significantly larger than the intensity obtained during only the gas discharge. The latter can be explained by the increased density of the preliminarily formed plasma due to ionization of evaporated atoms of the wall material. At $t = t_1$, the imploding wall reaches the vicinity of the axis, resulting in the sharp increase in the plasma density and temperature, and correspondingly in the intensity of radiation.

Let us estimate the mass velocity of the capillary material U_0 at $R_0 = 1\,mm$. Taking into account the dependence[11] of the radius of the imploding cylindrical wall versus time as

$$r(t) = R_0 \cdot \left(1 - \frac{t - t_0}{t_1 - t_0}\right)^{0.78}, \qquad (1)$$

one obtains the velocity of the capillary wall implosion at $t = t_0$

$$U_0 = -\left.\frac{dr}{dt}\right|_{t_0} = \frac{0.78 R_0}{t_1 - t_0}. \qquad (2)$$

Now, using the experimental values $t_0 \sim 6.85 \pm 0.05\,\mu s$ and $t_1 \sim 7.6 \pm 0.1\,\mu s$, one obtains that for the time delay $(t_1 - t_0) = 750 \pm 150\,ns$, the velocity of the inner boundary of the capillary is $U_0 \sim 1000 \pm 200\,m/s$. This velocity, due to formation of rarefaction wave, relates to the velocity U_q of the quartz material as $U_0 = 2U_q$, resulting in $U_q = 500 \pm 100\,m/s$.

Now one can estimate the velocity U_{q1} of the quartz material at the outer wall of the capillary behind the front of the converging shock wave propagating in quartz. The change in the velocity of this wave versus the radius can be estimated using the Whitham approach.[12] Namely, for a cylindrical geometry and $R_q = 1.5\,mm$, the material's velocity behind the shock wave front is $U_{q1} = U_q \times (R/R_q)^{0.5} = 410 \pm 80\,m/s$. This velocity and EOS for quartz can be used to determine the pressure P_q at $R_q = 1.5\,mm$

$$U_{q1} = \sqrt{(P_q - P_0)(v_0 - v_q)}, \qquad (3)$$

where $P_0 = 10^5\,Pa$ is the normal pressure, $v_0 = 1/\rho_{q0}$ and $v_q = 1/\rho_q$ are the specific volumes of the quartz at normal pressure and behind the shock wave front, respectively, $\rho_{q0} = 2.2 \times 10^3\,kg/m^3$ is the normal density of quartz, and ρ_q is the density of compressed quartz. Using the equation of state for quartz[13]

$$P_q - P_0 = 9 \times 10^9 (\delta_q^{2.6} - 1), \qquad (4)$$

where $\delta_q = \rho_q/\rho_{q0}$ is the compression of the quartz, one can find that at $R_q = 1.5\,mm$, quartz compression and pressure are $\delta_q = 1.13$ and $P_q = (3.3 \pm 0.7) \times 10^9\,Pa$, respectively.

Now, considering that at the water-capillary boundary the same pressure is realized, one obtains: $P_w = P_q = (3.3 \pm 0.7) \times 10^9\,Pa$, where P_w is the pressure in water at $R = R_q = 1.5\,mm$. This pressure buildup occurs due to an incident converging SSW and a reflected SSW from the capillary. Using the

approach described in Ref. [14], i.e., the momentum and energy conservation laws and equations of state for quartz and water, one can calculate the pressure behind the incident converging SSW front at $R = 1.5$ mm: $P_{ssw} = (1.9 \pm 0.4) \times 10^9$ Pa.

Now let us consider the results of the 1D hydrodynamic simulations coupled with EOS of water[15] and accounting for the time of the SSW implosion. These results showed that the pressure behind the SSW reaches 3×10^9 Pa, which results in a pressure $P_w \sim 5 \times 10^9$ Pa because of the reflected wave formation. However, this value of pressure should lead to a velocity of the inner capillary wall of ~ 1500 m/s. The latter is significantly larger than the estimated velocity ($U_0 \sim 1000$ m/s).

This discrepancy can be related to the assumption of normal incidence of the SSW with respect to the capillary's surface which is not correct in the case of a spherically converging SSW. In the latter case, one has to consider an oblique wave interaction with the capillary.[16] The angle of the SSW incidence depends on the wave's radius and, consequently, on the axial distance from the origin of implosion (see Fig. 7). The analytical solution of the pressure buildup is a rather complicated problem which is beyond the scope of the present paper.

In the case of quartz capillary, the coefficient related to the increase in the pressure because of reflected wave formation is changing from ~ 1 (SSW tangential incidence at $R_{SSW} \gg R_q$) to ~ 1.7 (SSW normal incidence at $R_{SSW} \approx R_q$). Considering spherical SSW, one obtains that the pressure $P_{ssw} \geq 2.3 \times 10^9$ Pa is realized behind its front at $R \leq 1.8$ mm corresponding to axial distance of $|z| \leq 1$ mm from the origin of implosion (see Fig. 7). The partial reflection of the incident SSW leads to increase in pressure $P_w < P_w^{max}$ ($P_w^{max} \sim 4 \times 10^9$ Pa at $R = 1.8$ mm and axial distance $|z| = 1$ mm corresponds to the case of the SSW normal incidence). Thus, the pressure $P_w = (3.3 \pm 0.7) \times 10^9$ Pa, required for wall implosion with velocity of ~ 1000 m/s, is realized at the water-quartz boundary allowing observation of the plasma enhanced light emission.

Let us note that an adiabatic compression of the plasma by an imploding capillary wall leads to an increase in the temperature of the plasma too. Assuming adiabatic compression 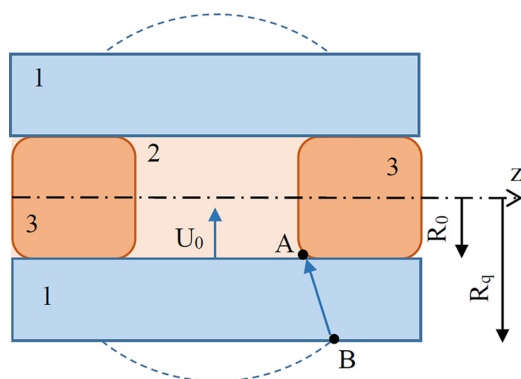of an ideal monoatomic gas, one can estimate the increase in the temperature as: $T = T_0(R_0/R)^{2(\gamma-1)}$ (where $\gamma = 1.67$ is the adiabatic index) resulting in a temperature >60 eV at $R < 100\,\mu m$ for $T_0 = 3$ eV at $R_0 = 1$ mm.

Thus, one can conclude that 1D hydrodynamic simulations that consider the SSW uniform convergence predict the correct range of the pressure behind the SSW front. Hence, from the known pressure of the SSW at such a small radius, one can better model its following evolution and calculate the water parameters of pressure and temperature in the vicinity of the SW implosion.

V. SUMMARY

In the present experimental research, the parameters of the plasma preliminarily formed in the capillary placed at the equatorial plane of the converging SSW were studied using time-resolved OES. The electrical explosion of a spherical wire array in water was used to produce this converging SSW. The evolution of the plasma density was studied using the Stark broadening of the spectral lines H_α and C II. It was found that, because of the compression of the plasma by the converging SW, the plasma electron density increases from 3×10^{17} cm^{-3} up to 5.5×10^{17} cm^{-3} during 250–300 ns. The compression probably continues farther, but the investigated spectral lines merge with the rising continuing radiation and this limits the analysis of the Stark FWHM of the spectral lines obtained. Using a simplified model, the velocity of the converging capillary wall and the pressure at the outer wall of the capillary were estimated. The results obtained indicate an oblique SSW interaction with the capillary which coincides with the assumption of spherically converging SSW.

ACKNOWLEDGMENTS

[1]V. E. Fortov and I. T. Iakubov, *The Physics of Non-Ideal Plasma* (World Scientific, Singapore, 2000).

[2]E. V. Krivitskii, *Dynamics of Electrical Explosion in Liquid* (Naukova Dumka, Kiev, 1983).

[3]D. Veysset, T. Pezeril, S. Kooi, A. Bulou, and K. A. Nelson, Appl. Phys. Lett. **106**, 161902 (2015).

[4]Ya. E. Krasik, S. Efimov, D. Sheftman, A. Fedotov-Gefen, O. Antonov, D. Shafer, D. Yanuka, M. Nitishinskiy, M. Kozlov, L. Gilburd, G. Toker, S. Gleizer, E. Zvulin, V. Tz. Gurovich, D. Varentsov, and M. Rodionova, IEEE Trans. Plasma Sci. **44**, 412 (2016).

[5]T. Pezeril, G. Saini, D. Veysset, S. Kooi, P. Fidkowski, R. Radovitzky, and K. A. Nelson, Phys. Rev. Lett. **106**, 214503 (2011).

[6]O. Antonov, S. Efimov, V. Tz. Gurovich, and Ya. E. Krasik, Phys. Plasmas **22**, 053507 (2015).

[7]M. Nitishinskiy, S. Efimov, O. Antonov, D. Yanuka, V. Tz. Gurovich, V. Bernshtam, V. Fisher, and Ya. E. Krasik, Phys. Plasmas **23**, 042705 (2016).

[8]M. Gigosos and V. Cardenoso, J. Phys. B: At., Mol. Opt. Phys. **29**, 4795 (1996).

[9]H. R. Griem, *Spectral Line Broadening by Plasmas* (Academic Press, New York, 1974).

[10]A. Grinenko, V. Tz. Gurovich, and Ya. E. Krasik, Phys. Plasmas **14**, 012701 (2007).

[11]V. Ts. Gurovich and L. G. Fel, JETP Lett. **89**, 14 (2009).

[12]G. B. Whitham, *Linear and Nonlinear Waves* (Wiley, New York, 1974).

FIG. 7. A schematic model of the plasma compression in the capillary. *1*—capillary; *2*—plasma; *3*—electrodes; R_0 and R_q—inner and outer capillary radii, respectively; U_0—the velocity of the inner capillary wall; dashed line—front of a spherical SSW in water.

[13]F. A. Baum, L. P. Orlenko, K. P. Stanyukovich, V. P. Chelyshev, and B. I. Shekhter, *Physics of Explosion* (Moscow, Nauka, 1975).

[14]O. Antonov, S. Efimov, V. Tz. Gurovich, D. Yanuka, D. Shafer, and Ya. E. Krasik, J. Appl. Phys. **115**, 223303 (2014).

[15]O. Antonov, L. Gilburd, S. Efimov, G. Bazalitzki, V. Tz. Gurovich, and Ya. E. Krasik, Phys. Plasmas **19**, 102702 (2012).

[16]G. Ben-Dor, *Shock Wave Reflection Phenomena* (Springer-Verlag, Berlin, Heidelberg, 2007).